Synthesis and Structural Features of -Fluorocarbonyl Systems

CRAIG AARON FISHER

Appendix 1 - Additional Discussion

Table of Contents

A1.1. Chapter 3

A1.1.1. Literature Synthetic Route to Racemic Fluorolactam Methyl 3-fluoro-2-oxopiperidine-3-carboxylate 248

The synthesis of dimethyl fluoromalonate **73** from dimethyl malonate is well reported in the literature having been optimised in Durham (***Figure 1***).[1]

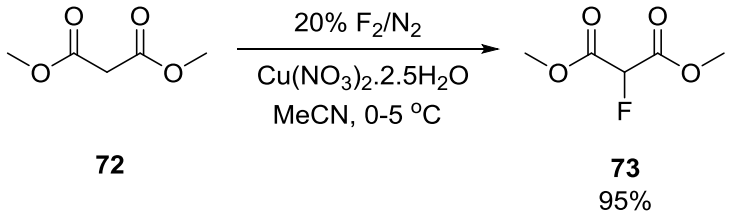

Figure 1 *- The synthesis of dimethyl fluoromalonate **73** from dimethyl malonate **72**.*

Bergmann, Cohen and Shani reported the synthesis of a fluorine substituted Michael addition product from diethyl fluoromalonate and acrylonitrile (***Figure 2***). Interestingly, they noted that the reaction gave erratic results and was not always reproducible, though they were able to report that, after distillation, isolation of the desired product in 65% yield along with unreacted fluoromalonate (27%).[2]

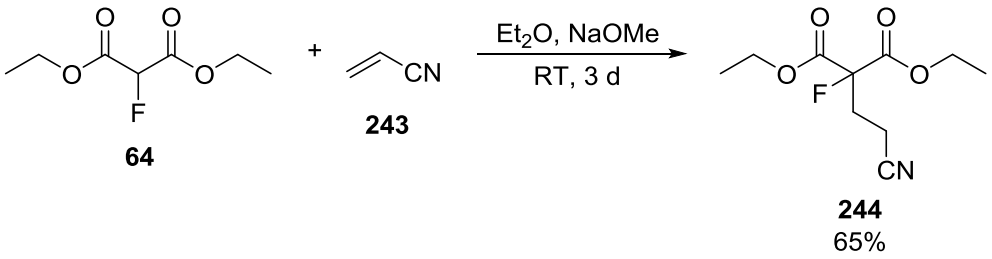

Figure 2 *- Michael addition reaction of diethyl fluoromalonate with acrylonitrile.*

The synthesis of analogous non-fluorinated lactam was reported in 1943 by Koelsch[3] and, subsequently, by Albertson and Fillman[4] who described a modified synthesis. Diethyl malonate undergoes a Michael addition reaction with acrylonitrile and is then reduced and cyclised using a Raney nickel catalyst under hydrogen (***Figure 3***).

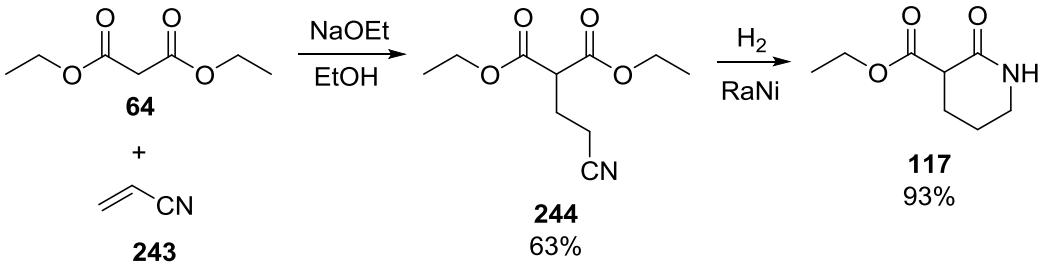

Figure 3 *- Synthesis of non-fluorinated heterocycle* ***117*** *from diethyl malonate and acrylonitrile using a Raney nickel (RaNi) catalyst for the reduction step.*

Related alkyl or aryl substituted malonates have been synthesised by similar procedures.[5,6]

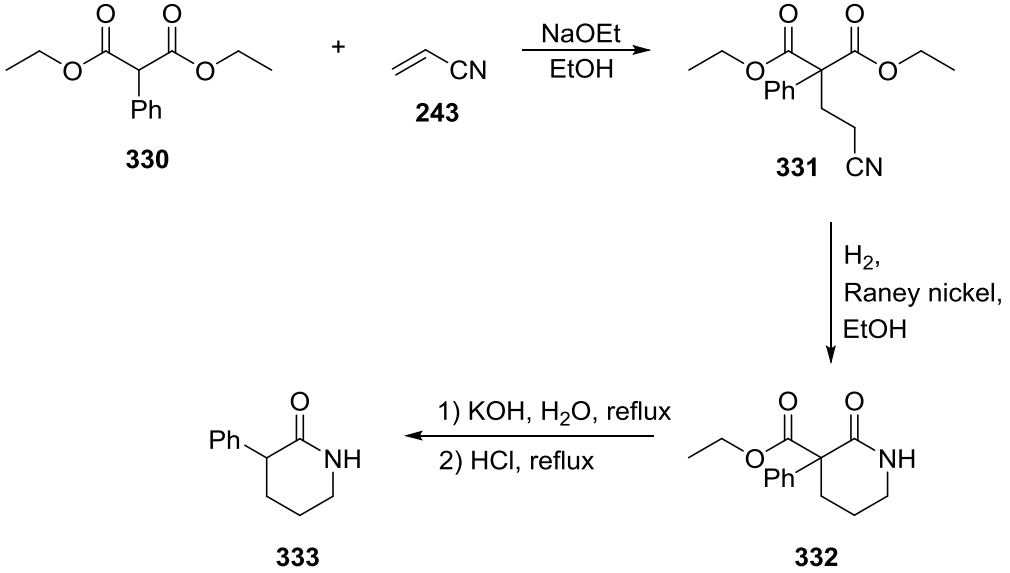

Figure 4 *- Synthetic route to phenyl substituted heterocyclic ester* ***332*** *from diethyl phenylmalonate* ***330*** *and acrylonitrile, plus an additional decarboxylation step.*

A1.1.2. Literature Supporting Desymmetrisation of Dimethyl fluoromalonate 73

In order for the product of this reaction to be chiral, one of the two malonate esters must be altered to differentiate it from the other ester. This could be, for example, via a hydrolysis reaction or conversion to a non-methyl ester.

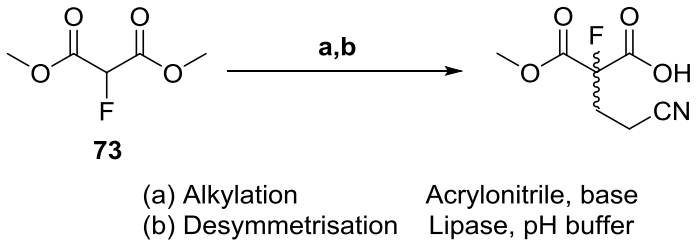

Figure 5 – *Possible chiral alkylation of dimethyl fluoromalonate **73**.*

Hong *et al*. reported the ligand catalysed chiral alkylation of a fluoromalonate diester giving the chiral product in 99% yield and 90% *ee* (***Figure 6***).[7]

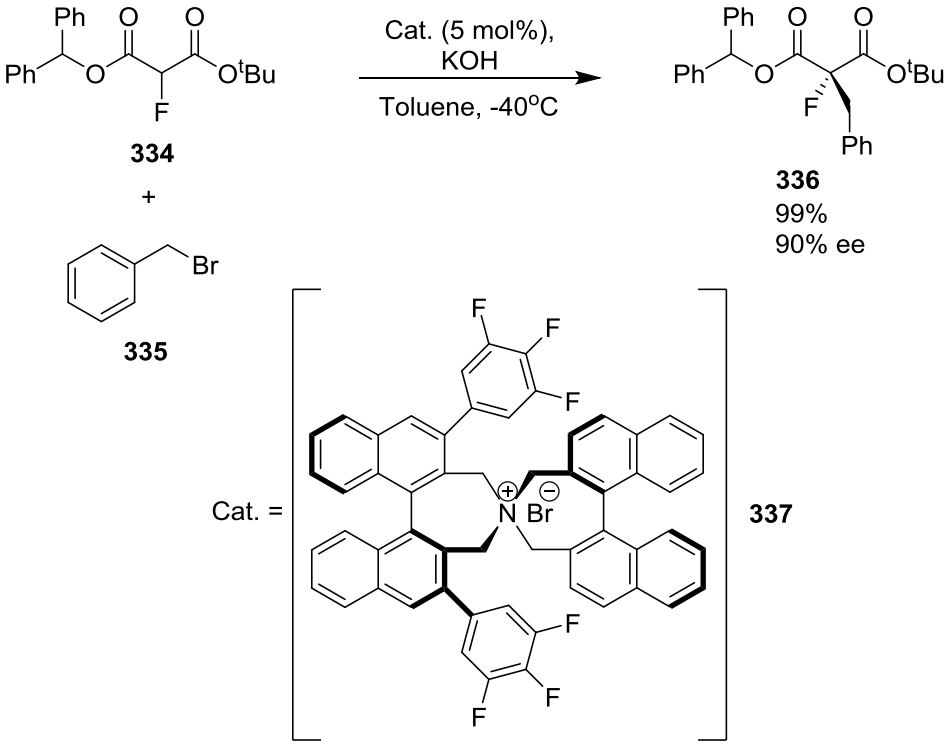

Figure 6 - *Ligand catalysed chiral alkylation reaction of fluoromalonate.*

Conversely, Reddy *et al*. reported the chiral fluorination reactions of alkylated malonate derivatives by NFSI catalysed by $Zn(OAc)_2$/DBFOX-Ph giving the chiral alkylated fluoromalonate derivative in good yield and *ee* (***Figure 7***).[8]

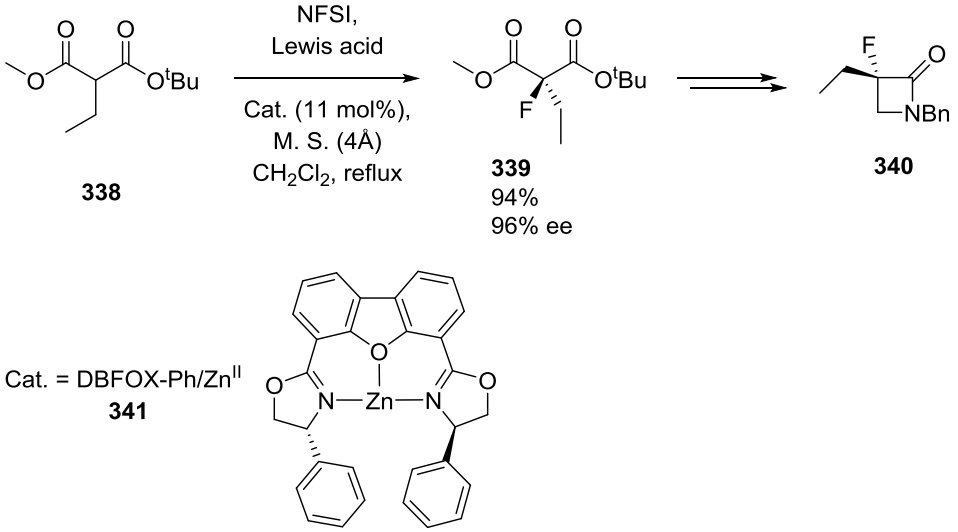

Figure 7 *- Chiral fluorination of an alkylated malonate derivative* ***338*** *by NFSI and a chiral zinc based ligand* ***341****, followed by steps to a chiral fluorolactam* ***340****.*

A1.1.3. Literature Supporting Desymmetrisation of Dimethyl (2-cyanoethyl)-2-fluoromalonate 246 or the Reduced Intermediate Dimethyl 2-(3-aminopropyl)-2-fluoromalonate, hydrochloride salt 247

Possible biocatalytic desymmetrisation of the related non-fluorinated malonate esters to alkylated fluoromalonate derivatives **246** and **247** to the related chiral hydrolysis products (***Figure 8***) has some literature precedent. The use of porcine liver esterase (PLE) has been reported for the synthesis of benzyl substituted heterocyclic systems from the prochiral diester in >99.5% *ee* (***Figure 9***).[9]

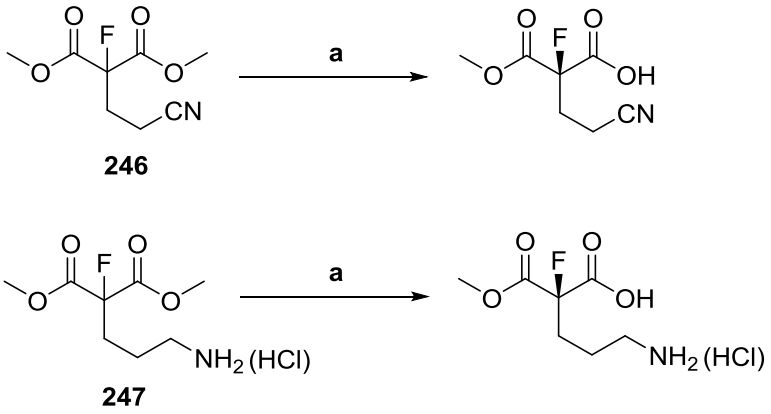

***Figure 8** – Possible desymmetrisation steps from alkylated fluoromalonate derivatives **246** and **247**.*

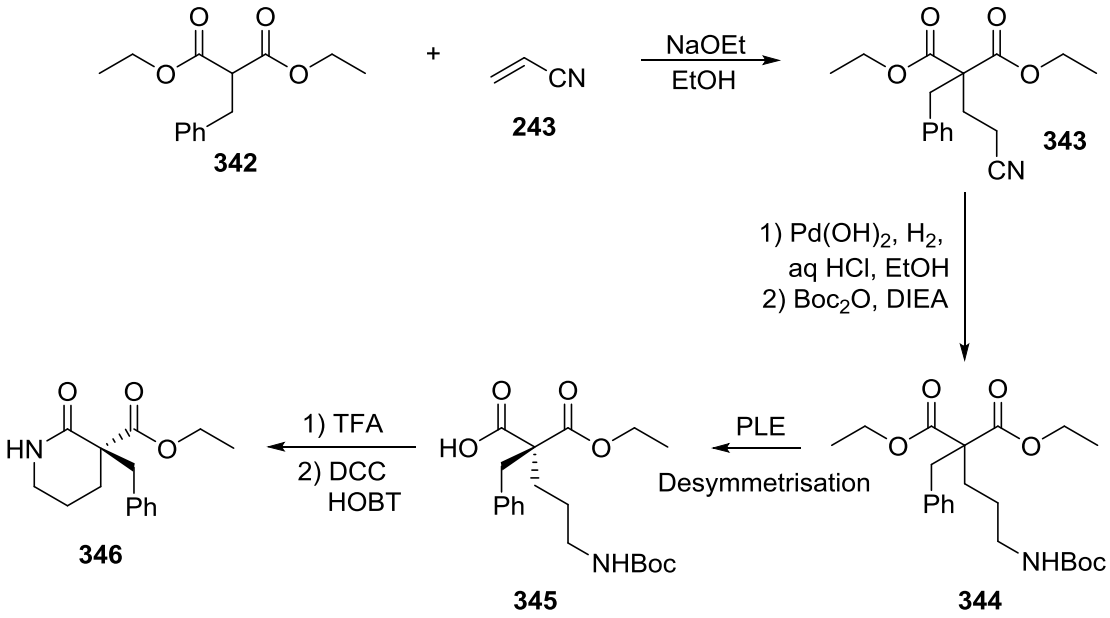

***Figure 9** - Reaction scheme to chiral heterocycle from substituted malonate and acrylonitrile via an enzyme catalysed process (DIEA is N,N-diisopropylethylamine, PLE is porcine liver esterase, TFA is trifluoroacetic acid, DCC is N,N'-dicyclohexylcarbodiimide, HOBT is hydroxybenzotriazole).*

Alternatively a chiral cyclisation reaction could potentially give the chiral fluorolactam (*S*)-**248** or a close derivative. This could potentially be telescoped to include a reduction reaction in the case of nitrile **246**.

The desymmetrisation of related diesters has been achieved by use of a chiral phosphoric acid catalyst to yield (non-fluorinated) enantioenriched lactone analogues (***Figure 10***), derivatives of which are found in drugs which have been shown to exhibit acetylcholinesterase inhibition and anticancer properties.[10] The diester was prepared by an alkylation reaction with the unsubstituted malonate. The chiral product was isolated in 97% yield and 98% *ee*.

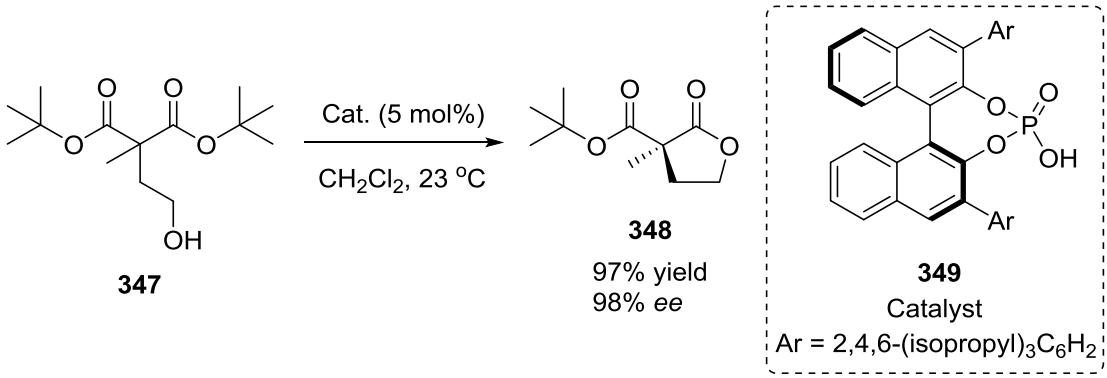

Figure 10 - *Desymmetrisation of a disubstituted diester **347** by use of a chiral catalyst.*

Although asymmetric synthesis with chemical catalysts may overcome some of the issues that the use of enzymes in biocatalysis may face (e.g. poor selectivity, instability of catalyst and difficulty recovering and reusing the enzyme) bulky inorganic catalysts tend to be expensive, even if only a small amount is required for catalysis.

Recent literature reports the desymmetrisation of an alkylated malonate derivative using commercially available Pig Liver Esterase (PLE) as a catalyst in the synthesis of a chiral monoester in good yield (68%) and excellent *ee* (97%) (***Figure 11***).[11]

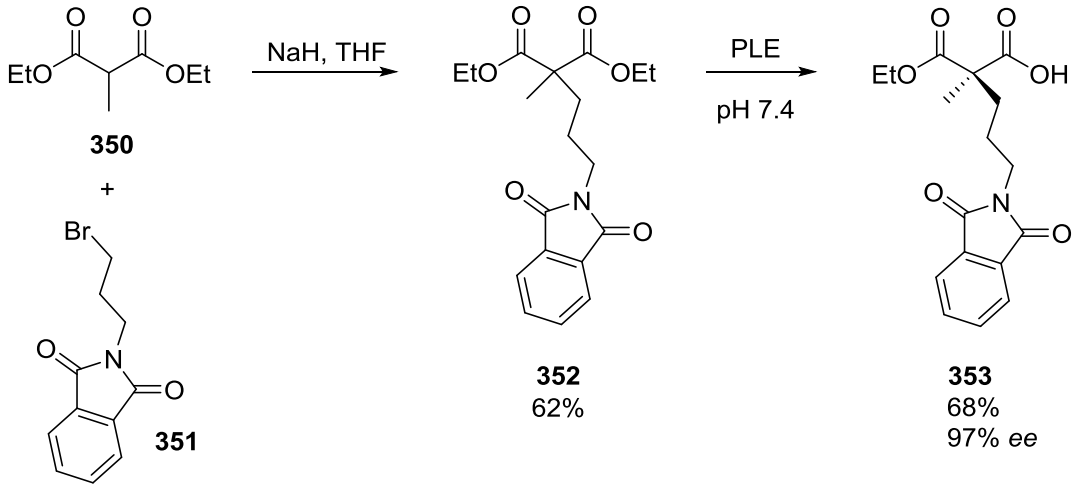

Figure 11 *- The literature synthetic route to a chiral malonate derivative* ***353*** *from an alkylated intermediate using Pig Liver Esterase (PLE) to give the product in good yield and excellent ee.*

Hydrolysis reactions of salt **247** were then investigated. Gutman *et al.*[12] had previously investigated the use of PLE and other enzymes in the synthesis of lactams by aminolysis of aminoesters (***Table 1***) but were only able to induce enantioselectivity in one example (entry **355d** in ***Table 1***) and only 23% *ee* was obtained.

Table 1 *– The intramolecular aminolysis of aminoesters catalysed by crude pancreatic porcine lipase.*

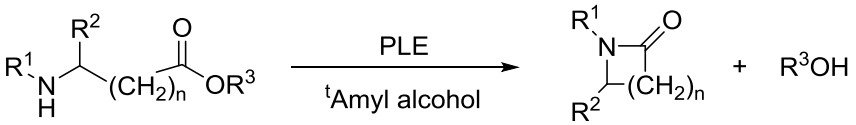

354a-h **355a-h**

Entry	R^1	R^2	R^3	n	Time /days	Enzymatic conversion /%
355a	H	H	CH_2CH_3	1	7	0
355b	H	CO_2Et	CH_2CH_3	2	2	50
355c	H	H	$CH(CH_3)_2$	2	3	45
355d	H	CH_3	$CH(CH_3)_2$	2	6	40
355e	CH_3	H	$CH(CH_3)_2$	2	6	30
355f	H	H	$CH(CH_3)_2$	3	4	80
355g	CH_3	H	$CH(CH_3)_2$	3	5	40
355h	H	H	$CH(CH_3)_2$	4	7	10

The authors suppressed the substantial background uncatalysed cyclisation by using sterically hindered isopropyl esters and tertiary amyl alcohol. They cited the example of methyl γ-aminobutyrate which cyclises in isooctane in 85% yield in 12 hours but the analogous isopropyl γ-aminobutyrate cyclises in tertiary amyl alcohol in only 2% yield after 7 days.

A1.1.4. Chiral Fluorination of Lactam 117

Two examples of chiral fluorination reactions of related lactams are discussed below.

The enantioselective late stage fluorination of a 6-membered lactam has been reported using a bulky chiral palladium based catalyst on >100 g scale (***Figure 12***).[13] The *ee* of the product was 44% which improved to >99% by chiral HPLC.

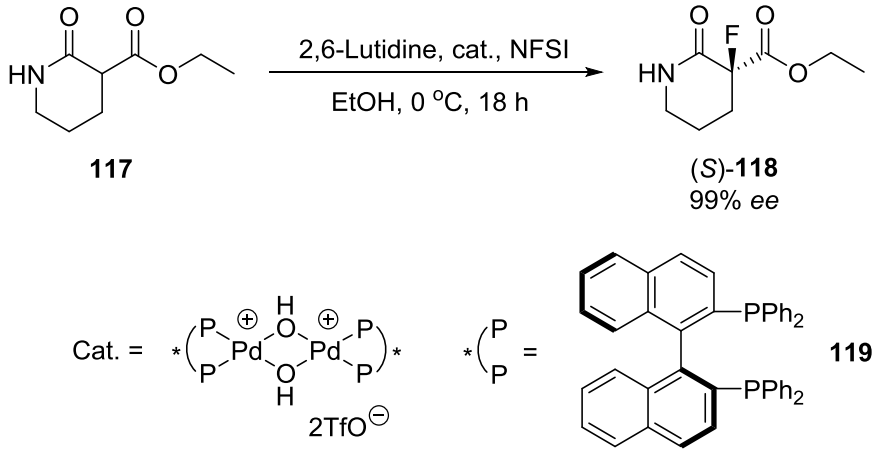

[(*S*)-(-)-2,2'-Bis(diphenylphosphino)-1,1'-binaphthyl]palladium (II) dihydrate ditriflate

= (*S*)-BINAP-Pd(OTf)$_2$(H$_2$O)$_2$

Figure 12 *- Chiral late stage fluorination of 6-membered lactam* ***117*** *by NFSI using a chiral Pd based catalyst.*

This reaction was later modified and scaled up to 37.0 kg of amidoester starting material. Reaction with (+)-menthol followed by a palladium complex catalysed chiral fluorination step gave the diastereomeric fluoroamidoester in 68% yield and 100% *de* (***Figure 13***).[14]

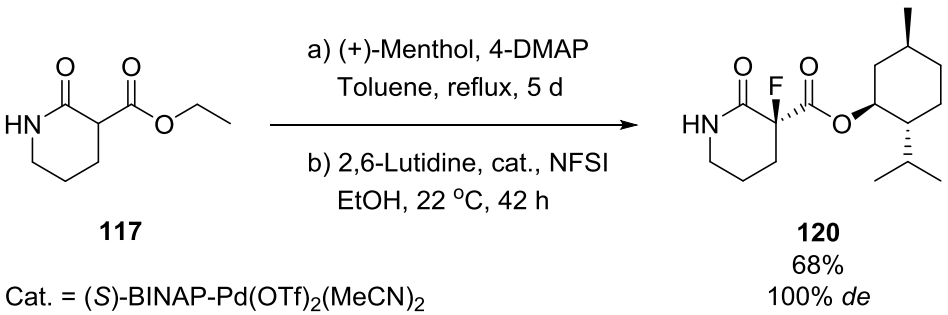

Figure 13 *- Transesterification and subsequent chiral late stage fluorination of a 6-membered lactam by NFSI using chiral Pd based catalyst on multikilo scale.*

A1.1.5. Initial screen of 56 enzymes against 248

***Table 2** – The percentage yields for the screening of the 56 hydrolases against **248**. (Work carried out by Nicky J. Willis).*

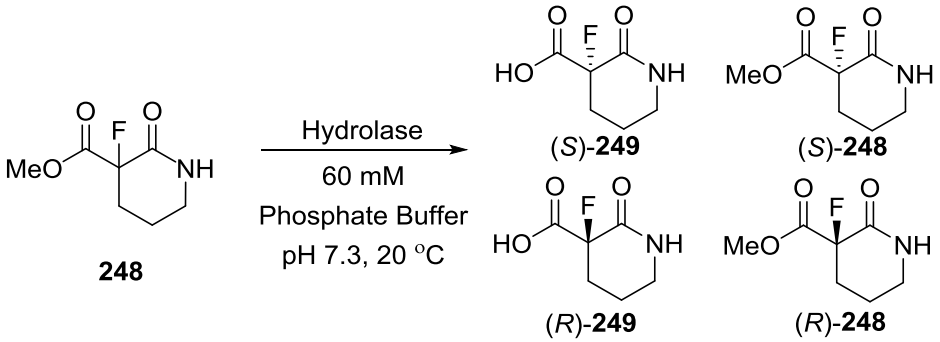

Entry	Hydrolase	Yield /%	Entry	Hydrolase	Yield /%	Entry	Hydrolase	Yield /%
1	JM X1	13	20	JM X20	17	39	JM X39	47
2	JM X2	3	21	JM X21	90	40	JM X40	5
3	JM X3	23	22	JM X22	5	41	JM X41	19
4	JM X4	2	23	JM X23	16	42	JM X42	3
5	JM X5	57	24	JM X24	59	43	JM X43	66
6	JM X6	2	25	JM X25	4	44	JM X44	39
7	JM X7	17	26	JM X26	3	45	JM X45	53
8	JM X8	2	27	JM X27	2	46	JM X46	2
9	JM X9	2	28	JM X28	2	47	JM X47	12
10	JM X10	3	29	JM X29	4	48	JM X48	50
11	JM X11	2	30	JM X30	23	49	JM X49	3
12	JM X12	42	31	JM X31	24	50	JM X50	28
13	JM X13	4	32	JM X32	13	51	JM EST 101	8
14	JM X14	30	33	JM X33	3	52	JM EST 102	100
15	JM X15	20	34	JM X34	3	53	PLE	100
16	JM X16	9	35	JM X35	19	54	CAL-B 10,000	51
17	JM X17	2	36	JM X36	0	55	PSL	0
18	JM X18	2	37	JM X37	14	56	Codexis EST002	99
19	JM X19	24	38	JM X38	16			

Yield Key /%	0-10	10-25	25-50	50-60	60-100

A1.1.6. Metric Analysis of Further Optimised Hydrogenation and Cyclisation Steps

The metric values for the GSK optimised syntheses of salt **247** and fluorolactam (*S*)-**248** are shown below.

Salt **247** was synthesised in 84% yield and had an AE of 100, an RME of 73.7 and a total PMI of 12.0 (***Figure 14***). The subcategories' MI values are; Reaction MI = 5.2, Solvent MI = 10.1 and Work-up MI = 6.8. The majority of the PMI is contributed by the solvent category and, overall, the optimised PMI of this process is very low.

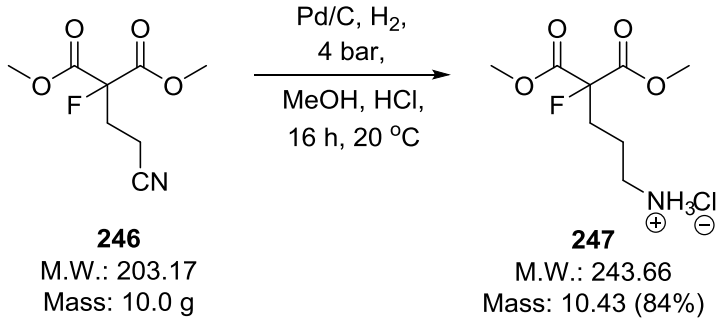

246
M.W.: 203.17
Mass: 10.0 g

247
M.W.: 243.66
Mass: 10.43 (84%)

Yield	84
AE	100
RME	73.7
PMI total	12.0
PMI Reaction	5.2
PMI Solvents	10.1
PMI Workup	6.8

Materials used in reaction: Pd/C (2.62 g), hydrogen (M.W.: 2 x 2.02, 1.0 g, assuming 3 L gas volumes (autoclave + storage tank) at 4 bar and 20 °C) conc. HCl (M.W.: 36.45, 5.82 g), MeOH (81.7 g).

Materials used for workup and isolation: Acetone (23.7 g).

$$AE = \frac{243.66}{203.17 + 4.04 + 36.45} \times 100 = \mathbf{100.0}$$

$$RME = \frac{10.43}{10.0 + 2 + 2.15} \times 100 = \mathbf{73.7}$$

$$MI = \frac{2.62 + 5.82 + 10.0 + 1 + 81.7 + 23.7}{10.43} = \mathbf{12.0}$$

***Figure 14**– Optimised synthesis and selected metric calculations of hydrochloride salt **247** from nitrile **246**.*

Chiral fluorolactam (*S*)-**248** was synthesised in 43% yield (99% *ee*) and had an AE of 35.9 and an RME of 31.5 (***Figure 15***). These metrics are rather low due primarily to the 50% maximum yield of the resolution since the undesired enantiomer (*R*)-**249** is wasted. The PMI for this step was 132.0, 126.6 of which came for the solvent category (246 g buffer solution for 10 g salt **247**). The solvent for this step is water and, though used in large volumes, is not particularly environmentally harmful.

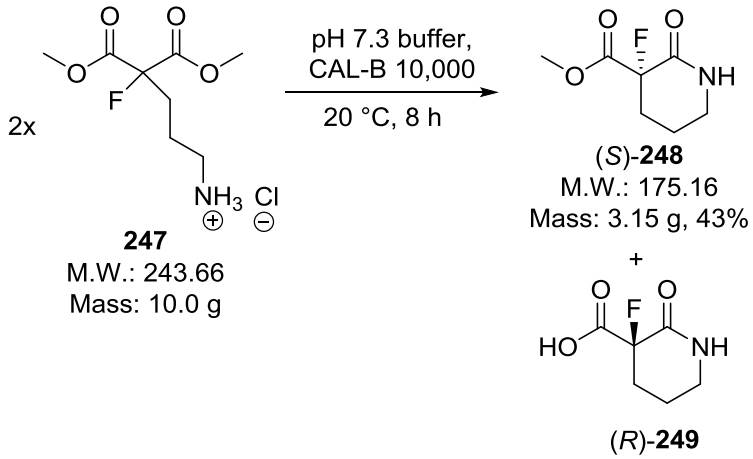

Yield	43
AE	35.9
RME	31.5
PMI total	132.0
PMI Reaction	110.1
PMI Solvents	126.6
PMI Workup	21.9

Materials used in reaction: 0.06 M Na2HPO4 : 0.06 M KH2PO4 buffer (assume overall 246 mL, assume d = 1.0 g/mL, 246 g), 05 M NaOH solution (assume 1 equivalent NaOH, 82 mL, 83.6 g solution), Fermase immobilised CAL-B 10,000 (7.2 g).

Materials used for workup and isolation: Water (30 g), formic acid (31.2 g), acetone (7.9 g).

$$AE = \frac{175.16}{2 \text{ x } 243.66} \times 100 = \mathbf{35.9}$$

$$RME = \frac{3.15}{10.0} \times 100 = \mathbf{31.5}$$

$$MI = \frac{246 + 10 + 83.6 + 7.2 + 30 + 31.2 = 7.9}{3.15} = \mathbf{132.0}$$

Figure 15** – Optimised synthesis and metric calculations of fluorolactam (S)-**248** from hydrochloride salt **247.

A1.1.7. Overall Metrics Comparisons between the Literature Synthetic Process and the Alternative Optimised Synthetic Process

With the telescoped synthesis of nitrile **246** from dimethyl malonate via fluoromalonate **73** optimised in Durham and the syntheses of salt **247** from nitrile **246** and chiral fluorolactam (*S*)-**248** from salt **247** developed in collaboration with GSK, the overall metrics analysis of the optimised process were compared with the literature process.

The metrics for the Durham/GSK process are as follows. Full details and calculations can be found in the supporting information of the related publication.[15]

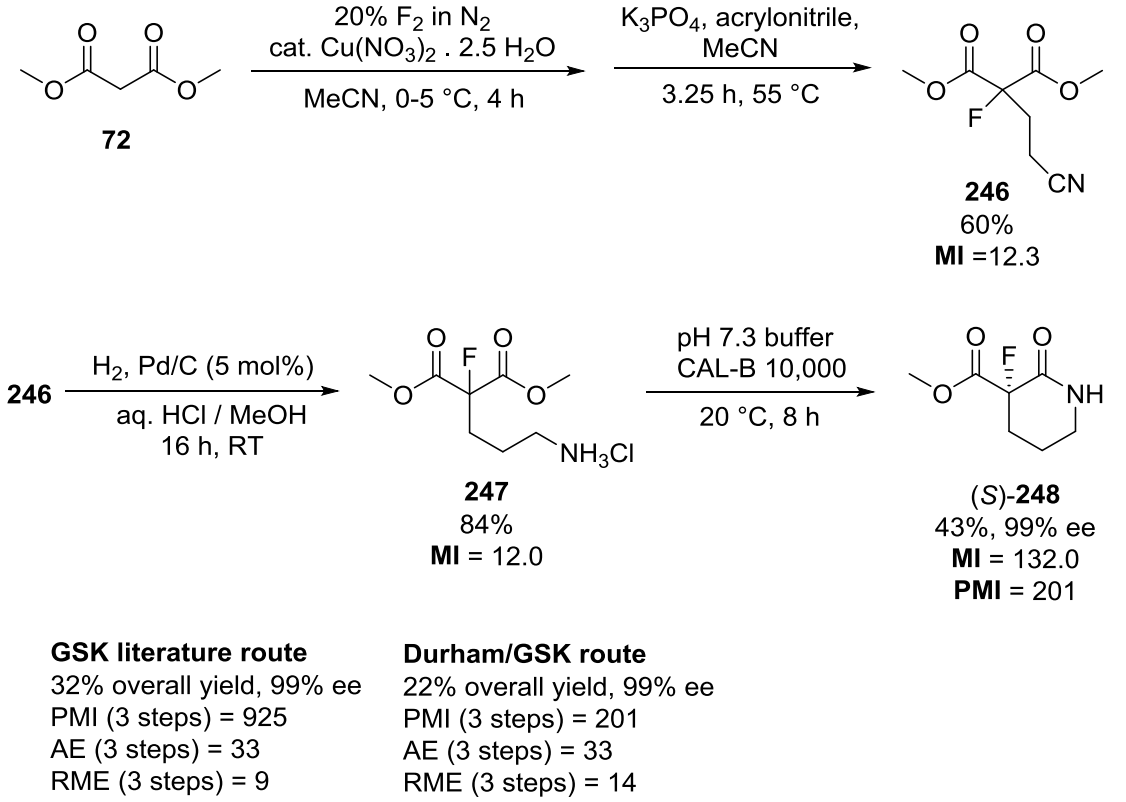

***Figure 16** – The optimised synthesis of fluorolactam (S)-**248** from dimethyl malonate.*

***Table 3** – Selected metric data for the optimised synthesis of fluorolactam (S)-**248**.*

Dimethyl malonate to **246**	
Yield	60
AE	90.1
RME	51.1
PMI total	12.3
PMI Reaction	8.7
PMI Solvents	6.7
PMI Workup	3.6

Nitrile **246** to salt **247**	
Yield	84
AE	100
RME	73.7
PMI total	12.0
PMI Reaction	5.2
PMI Solvents	10.1
PMI Workup	6.8

247 to lactam (*S*)-**248**	
Yield	43
AE	35.9
RME	31.5
PMI total	132.0
PMI Reaction	110.1
PMI Solvents	126.6
PMI Workup	21.9

Overall Process	
Yield	22
AE	33.2
RME	14.0
PMI total	201.2
PMI Reaction	146.6
PMI Solvents	179.0
PMI Workup	54.7

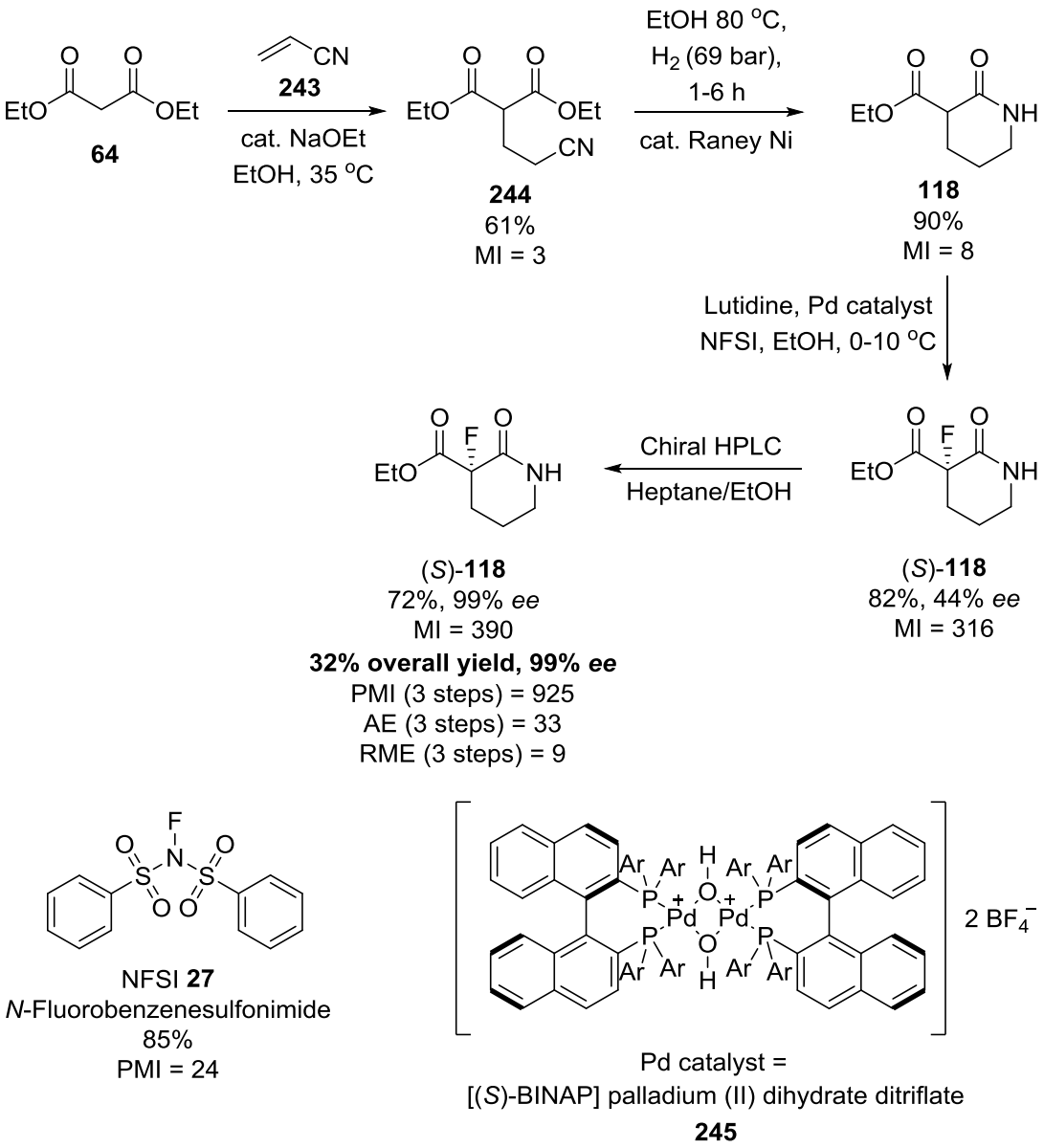

Figure 17 – *Literature route to chiral fluorolactam (S)-**118** (the ethyl ester of target (S)-**248**) with metric calculations.*

A1.2. Chapter 5

The following tables display results from the CRED screening reactions.

Table 4 displays the initial distribution of products and unreacted ketone for each CRED solution.

Table 4 – *Initial results of CRED screening of ethyl 2-fluoroacetoacetate* ***282.***

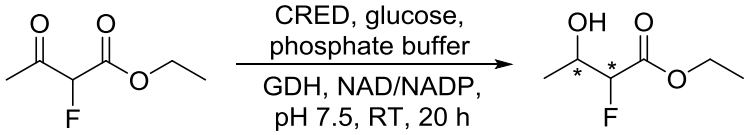

282 **283**

CRED	GC Peak Area /%				
	Ketone	**Alcohol 1**	**Alcohol 2**	**Alcohol 3**	**Alcohol 4**
1	9.2	4.4	5.9	80.5	0
2	0.3	30.5	1.8	8.1	59.7
3	0.3	38.5	0	11.1	50.1
4	1.7	40.4	2.5	6.9	47.9
5	0.3	2.2	5	92	0
6	0.6	0	6.9	7.6	85.6
7	40.2	26	1	5.3	27.3
8	0.2	39.1	0	60.7	60.7
9	0.2	39.8	0	59.7	0
10	0.1	40.8	0	58.7	0
11	1.4	0	40.9	56.7	0
12	0.1	0	8.2	91.3	0
13	0.1	3.2	2	30.3	64.1
14	0.1	11.6	0.7	87.7	0
15	0.3	15.2	0.4	83.4	0
16	50.5	16.7	4.3	5.8	22.5
17	0.2	3	0.2	96.6	0
18	0.2	0.3	1.1	0.2	98.2
19	0.1	60.1	5.3	3.4	30.7
20	0.5	31.4	3	18.9	45
21	34.9	31.4	0.8	8.6	24
22	66.7	15.6	0.5	16.9	0
23	0.3	7.7	0.2	91.9	0
24	1.7	0	11.8	0	83.3
25	0.3	90.1	0	9.4	0
26	54.1	0	35.5	0.9	9.3
27	0.3	82	0	17.5	0
28	57	22.3	0	20.5	0

29	5.3	0	82.9	0	11.1
30	0.1	0.1	1.7	2	95.9
31	61.7	22.2	0.7	1.6	13.7
32	0.3	91.5	0	8.3	0
33	0.2	78.7	0	8	12.9
34	0.2	19.4	10.2	17.4	52.7
35	0.2	76.8	0	10.4	12.3
36	34.2	39.7	0	1.2	7.4
37	55.4	17.5	10.1	5.8	10.9
38	62.7	29.2	0	7.9	0
39	0.4	53.2	2.3	30.1	13.7
40	0.3	20.2	74.9	74.9	0
41	0.1	29.2	70.7	0	0
42	0.2	93.36	0	6.3	0
43	0.3	87.3	0	12.1	0
44	0.2	0.7	4.5	94.1	0
45	0.3	0	36.2	6.1	57.4
46	71.7	18	1.1	1.4	7.7
47	6.8	80.6	0	2.9	9.6
48	52.6	21.6	4	21.5	0
49	80.4	11.4	0.8	0.9	6.3
50	0.5	94.1	0	5.3	0
51	0.1	45.8	3.8	50.1	0
52	69.8	15.2	1.2	4.5	9.2
53	29.2	36.4	8.2	5.5	20.5
54	46.6	15.6	2.6	33.1	0
55	0.3	83.4	15.8	0	0
56	1.5	62.5	35.8	0	0
57	0.1	38.1	61.8	0	0
58	0.2	7.9	19.2	11.1	60.9
59	0.3	4.1	94.5	0	0
60	34.9	27.2	2.1	2.4	33.4
61	91.3	5.8	0	2.7	0
62	50.5	31.5	1.6	16.2	0
63	0.2	10.5	0.7	88.6	0
64	39.3	27.1	5	3.2	25.1
65	0.3	51.2	0	48.3	0
66	0.1	56.5	0	43.1	0
67	0.1	60.3	0	39.6	0
68	35.8	40.5	0	23.5	0
69	14.7	53.7	13.3	1.5	16.6
Blank	91.3	5.8	0	2.7	0

Table 5 *– Colour coding of entries which display selectivity above 50%.*

Isomer Excess /%	Colour
95-100	
90-94	
80-89	
70-79	
50-69	

Table 6 *– Colour coded entries exhibiting over 50% isomer excess.*

CRED	Isomer Excess /%			
	Alcohol 1	Alcohol 2	Alcohol 3	Alcohol 4
1			67.2	
5			84.7	
6				71.1
12			83.0	
14			75.4	
15			67.5	
17			93.4	
18				96.6
23			84.0	
24				70.0
25	80.6			
27	64.3			
29		70.0		
30				92.1
32	83.2			
33	57.6			
35	53.9			
42	87.0			
43	75.1			
44			88.8	
47	65.7			
50	88.7			
55	67.3			
59		90.3		
63			77.4	

A1.3. Chapter 6

A1.3.1. Miscellaneous Exclusions

The total number of entries is 144, not 143. This discrepancy arises because QALBIP (***Figure 18***) shows two independent molecules in its crystal structure. One molecule (QALBIP (A)) gives an F-C-C=O torsion angle of -175^{o} and has been included in this study. The other molecule (QALBIP (B)) exhibits significant distortion of the fluoroester moiety and so has been assigned to the 'disordered' category. QALBIP has therefore been included twice and so brings the total number of entries to 144 with 100 exclusions.

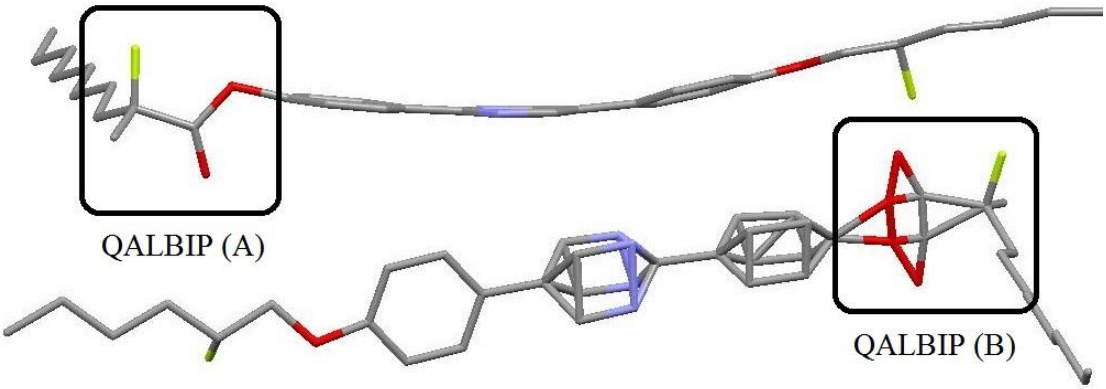

Figure 18 *– QALBIP consists of two independent molecules, one of which (QALBIP (B)) has been excluded from this study due to the disorder affecting the fluoroester moiety.*

A1.3.2. Further Examples of Cyclic α-Fluoroesters

ZUWYAT exhibits a *syn* F-C-C=O bond angle of -11^{o}. This can likely be attributed to the mix of sp^2 and sp^3 atoms in the heterocycle that leads to an unusual ring puckering (***Figure 19***).

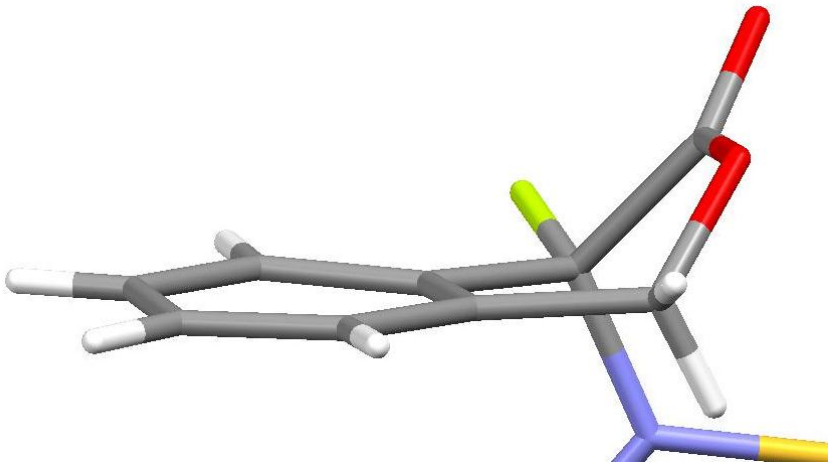

Figure 19 – *The mix of sp^2 and sp^3 atoms in the heterocycle moiety of ZUWYAT may lead to a smaller than expected F-C-C=O torsion angle than would be expected.*

VEKLUT also contains an aldehyde F-C-C=O moiety from the same fluorine atom and, as such, is a fluorodicarbonyl system. The fluoroaldehyde torsion angle is -114^{o} (***Figure 20***).

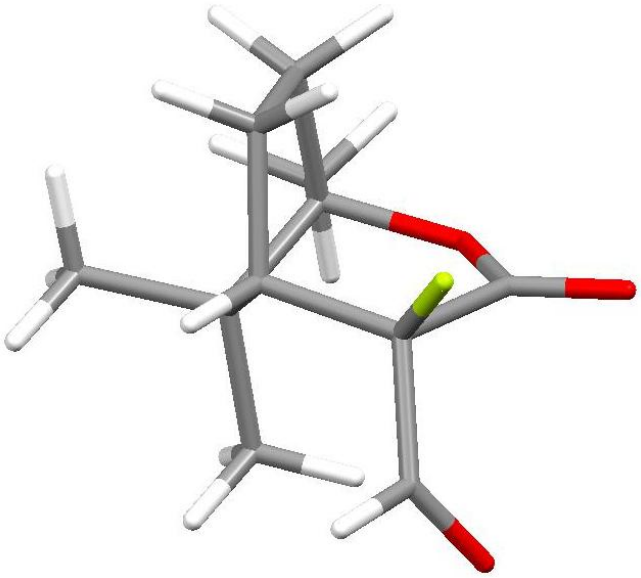

Figure 20 – *The molecular structure of VEKLUT also contains a fluoroaldehyde moiety.*

A1.3.3. Further Examples of α-Fluoroesters on a Ring System

TORPOH has three additional fluoroamide moieties that do not include the same fluorine atom as the fluoroester moiety (***Figure 21***).

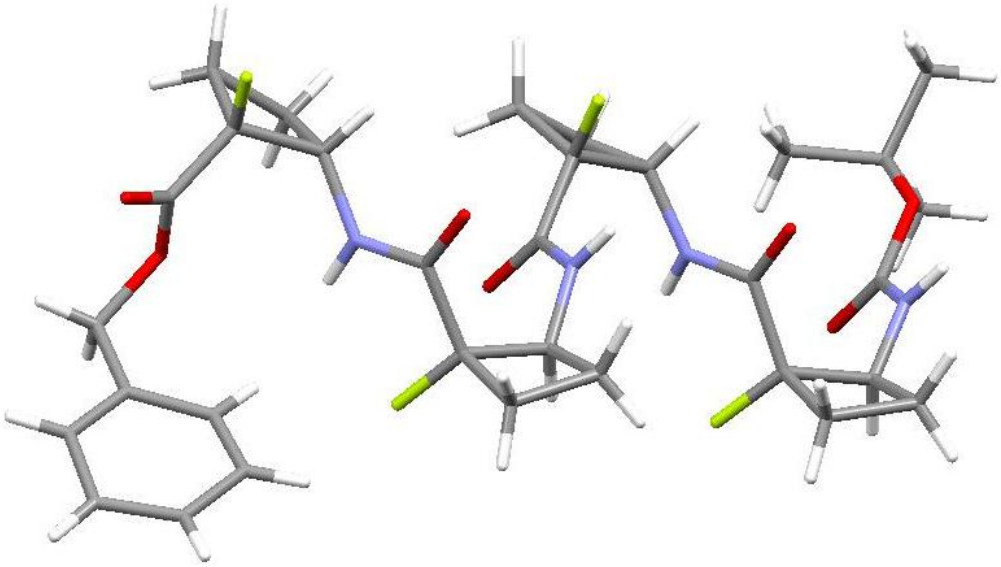

Figure 21 *– The molecular structure of TORPOH.*

LISMOQ exhibits *eclipsed* conformation. This is possibly due to steric hindrance between the bulky ^{t}butyl ester alkyl moiety and the adjacent bulky moiety (***Figure 22***).

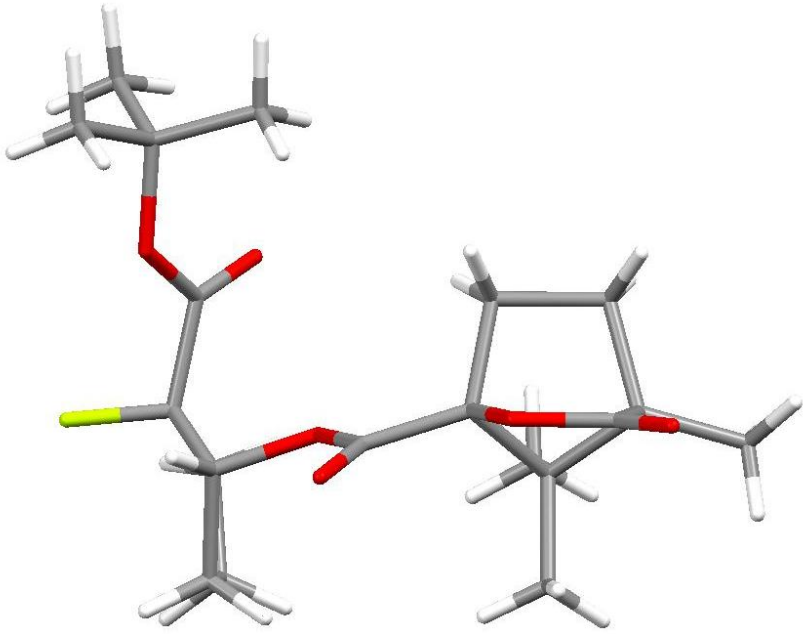

Figure 22 *– The molecular structure of LISMOQ.*

PIWVIC also exhibits *eclipsed* conformation. This may be a result of steric hindrance between the ethyl ester moiety and the nearby fluorophenyl moiety. Three intermolecular hydrogen bonding interactions are observed to involve the ester carbonyl oxygen, which may also lead to the *eclipsed* fluoroester conformation (***Figure 23***).

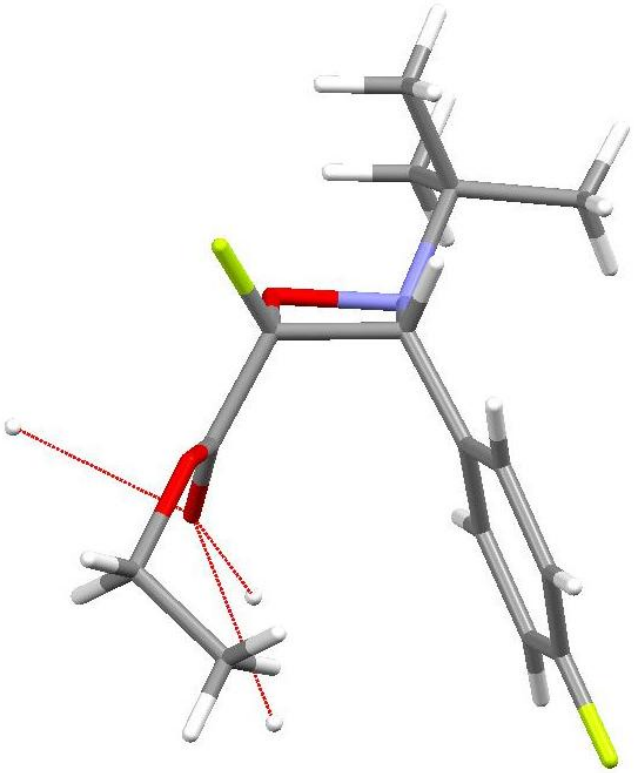

Figure 23 *– The molecular structure of PIWVIC.*

It is less clear whether WOLGAF and RUXZAM have any obvious interactions that could lead to an *anti* conformation, though WOLGAF features both a nitrile moiety and an amine moiety that interact and stack, leaving the ester moiety on the external face of the crystal (***Figure 24***). RUXZAM is a very bulky molecule and so likely exhibits steric hindrance involving the bulky fluoroester moiety (***Figure 25***).

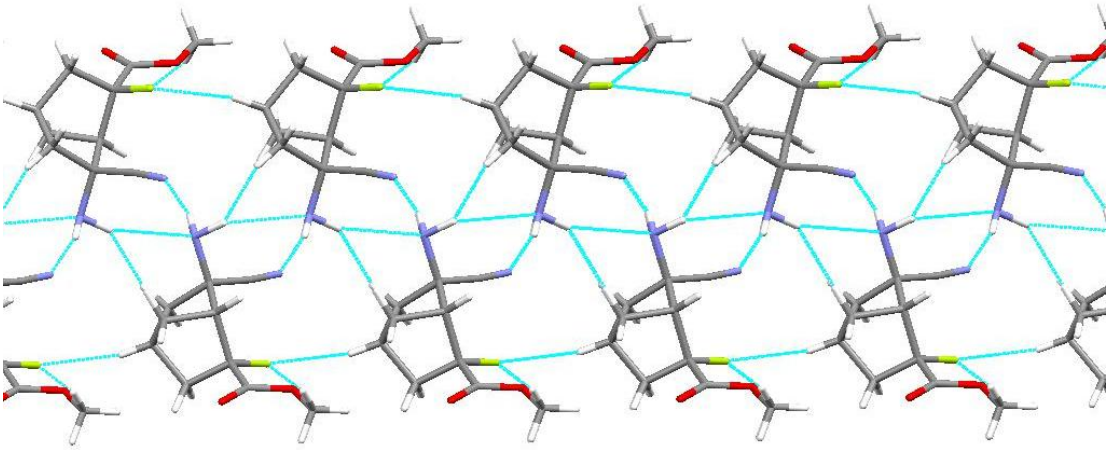

Figure 24 *– The molecular structure of WOLGAF.*

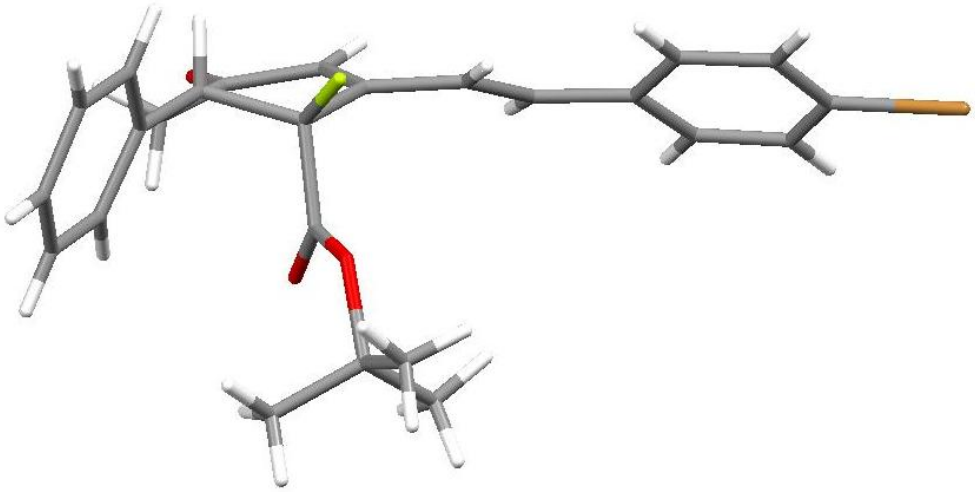

Figure 25 *– The molecular structure of RUXZAM.*

RUXZEQ exhibits intramolecular hydrogen bonding interactions between the fluoroester carbonyl oxygen and an adjacent hydroxyl moiety when in the *ant*i conformation which may strengthen the *anti* conformational preference observed in this structure (***Figure 26***).

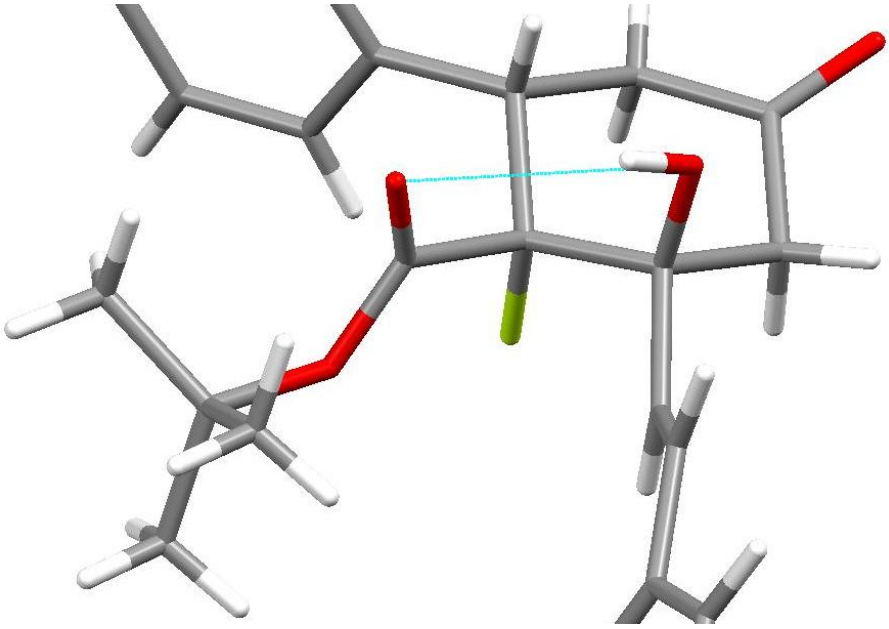

Figure 26 *– The molecular structure of RUXZEQ.*

A1.3.4. Further Example of an α-Fluorodicarbonyl on a Ring System

SUHBUT exhibits intermolecular interactions between the fluoroester carbonyl oxygen atoms and bromine atoms which may lead to an increased *anti* fluoroester conformational preference in this structure (***Figure 27***).

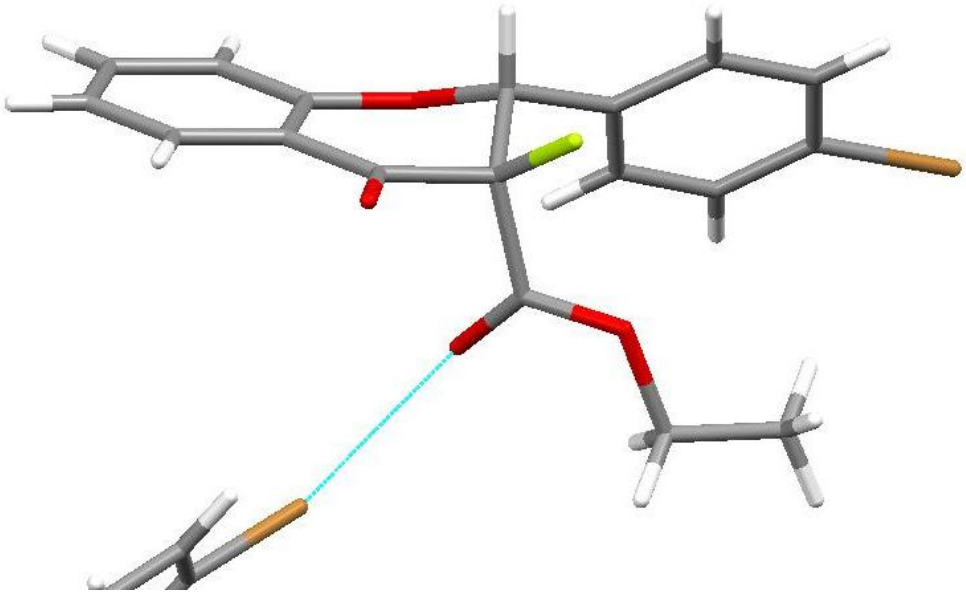

Figure 27 *– The molecular structure of SUHBUT.*

The remaining four entries with *anti* conformations exhibit a variety of interactions that may lead to their anti conformations, though there is more uncertainty regarding these structures.

A1.3.5. Exclusions and Further Examples of α-Fluorinated Monoacids

Exclusions- OHIJAR, OHIJAR01, OHIJAR02, OHIJAR03 and OHIJAR04 are all identical in chemical structure, though differ in conformation and crystal packing arrangement. Although all five are carboxylic acids instead of esters and so were not included in this section, OHIJAR03 was selected to be included in the carboxylic acid category because it had the lowest R-factor (***Figure 28***).

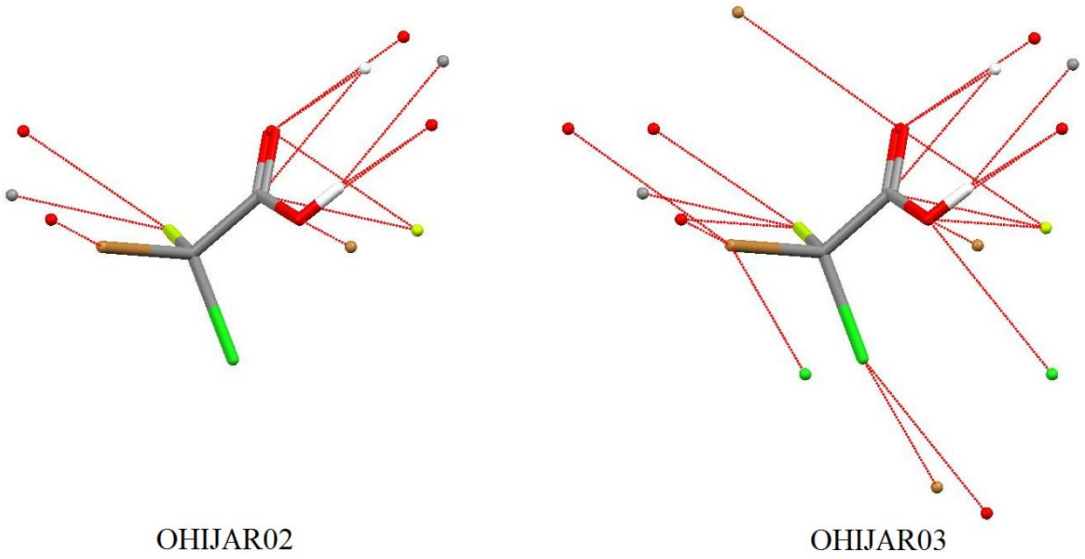

Figure 28 *– The crystallographically determined molecular structures of OHIJAR02 and OHIJAR03, including intermolecular interactions.*

The two *eclipsed* angles are from two independent molecules of the same structure (QUKHUZ) that features two fluoroacid moieties in close proximity to each other. The proximity of the two acid moieties may explain the unusual F-C-C=O torsion angle. The *eclipsed* fluoroacid moiety also exhibits intermolecular hydrogen bonding interactions that may explain the conformation (***Figure 29***).

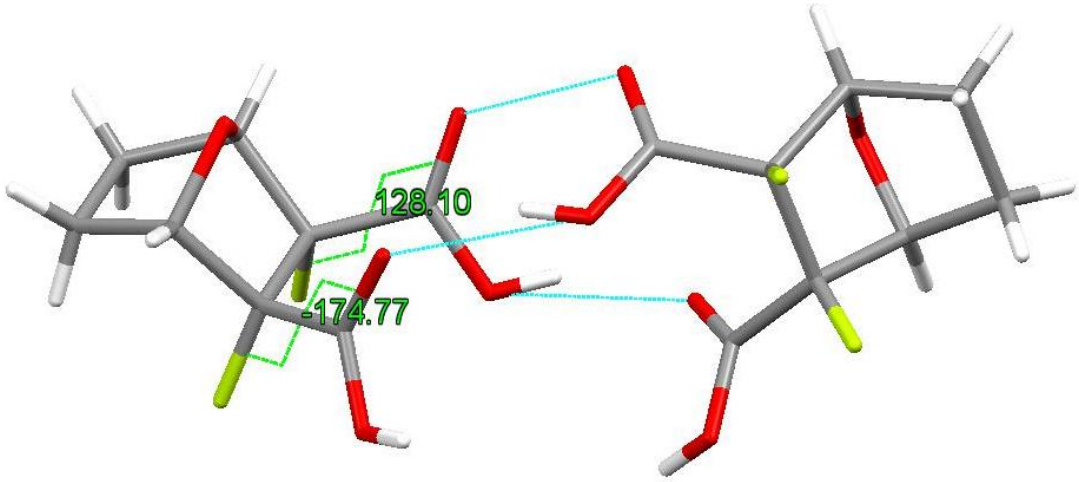

Figure 29 – *The molecular structure of QUKHUZ with selected hydrogen bonding interactions involving the eclipsed fluoroacid moiety.*

BAWHAI is a diacid but exhibits disorder in one of the two acid hydrogen atoms. As such, this torsion angle is indeterminate and has been omitted (***Figure 30***).

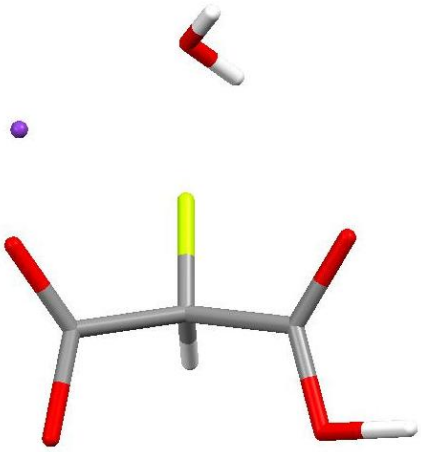

Figure 30 – *The molecular structure of BAWHAI exhibits disorder in one of the two fluoroacid moieties.*

A1.3.6. Exclusions from α-Fluoroamide Search

Both the CCDC's ConQuest software and online WebCSD search functions were used and the two sets of results were combined to form one definitive dataset for this study. It is of note that while minor discrepancies between the two search functions were observed in the fluoroester study, the discrepancy is considerably larger in this fluoroamide study. ConQuest returned 124 entries, whereas WebCSD only returned 57 of the combined total of 128 entries.

Additionally, not all 57 of these WebCSD entries were returned by ConQuest. Overall, only 53 (41%) of the total 128 entries appeared on both search functions. Furthermore, this combined dataset of 128 entries is known to be incomplete since a number of molecules that contain both fluoroester and fluoroamide moieties were identified by the search functions for the fluoroesters study but not for the fluoroamides study. Several of our own fluoroamide structures have been uploaded to the CSD but have not been identified by its search functions in this study. This study will only analyse structures returned by the search functions since the number of undetected fluoroamide structures is unknown. These discrepancies between the CSD's two search functions and also between the search functions and the CSD database itself highlight the fact that any statistical study of a database can only be as good as the search function used.

As of March 2016, the CSD searches returned 128 entries which, after inclusion of multiple independent molecules within a crystal structure, gave a dataset of 178 structures. Seven of these 178 entries had no 3D data available and so were excluded from this study whilst 13 structures exhibited disorder involving the fluoroamide moiety and so were excluded. A further nine structures were duplicates of other entries and so have also been excluded. Stereoisomers of molecules have been included (e.g. *cis/trans* isomers or *R* and *S* enantiomers of the same compound), it is only identical duplicates of a molecule which have been excluded. Consequently, these exclusions left a dataset of 149 structures to be analysed.

A1.3.7. Exclusions and Further Discussion of α-Fluoroamides

As with the α-fluoroesters described above, this category describes the simpler α-fluoroamide entries in the CSD and excludes cyclic fluoroamides, acyclic fluoroamides adjacent to ring systems that may hinder free rotation of the FC-CO bond and polycarbonyl derivatives. These exclusions are described subsequently.

The apparent *anti* preference of these structures is consistent with three additional entries not listed in this category. These three structures (LUHQOU, LUHQUA and LUHRAH) are primary amides but show F-C-C=O disorder between two different conformations and so they have been excluded. It is of note, however, that in the three structures, all six of the observed conformations are *anti* (***Figure 31***).

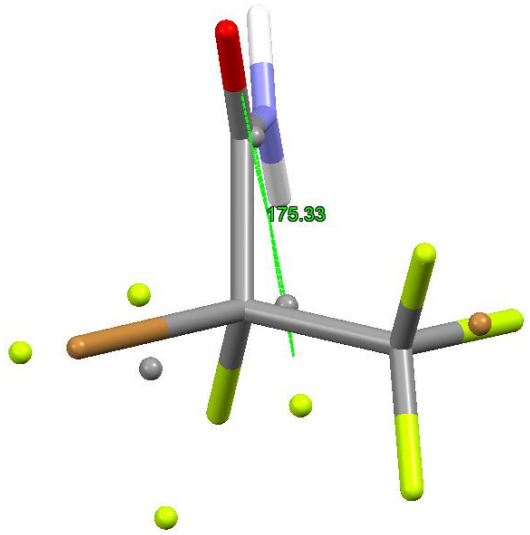

Figure 31 – *LUHQUA has an F-C-C=O bond torsion angle of 163 ^{o} and a secondary torsion angle of 175 ^{o} over the disordered site.*

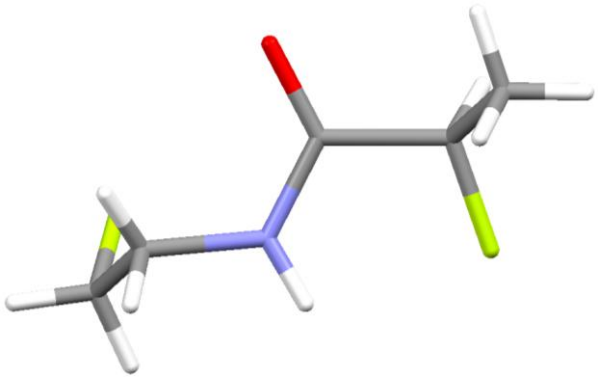

Figure 32 *– TUWWOX is an example of a secondary fluoroamide derivative. It has an F-C-C=O bond torsion angle of -177 ^{o}.*

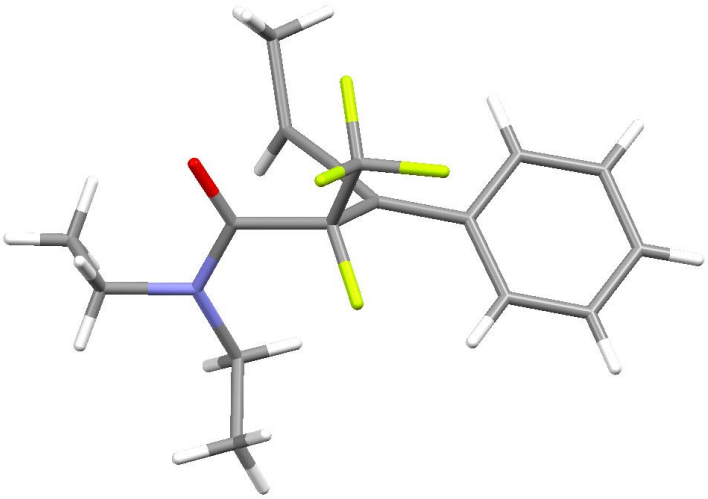

Figure 33 *– ISAFAJ is an example of a tertiary fluoroamide derivative. Its crystal structure has two independent molecules with F-C-C=O bond torsion angles of -126 ^{o} and 131^{o}.*

A1.3.8. Further Examples of α-Fluorolactams

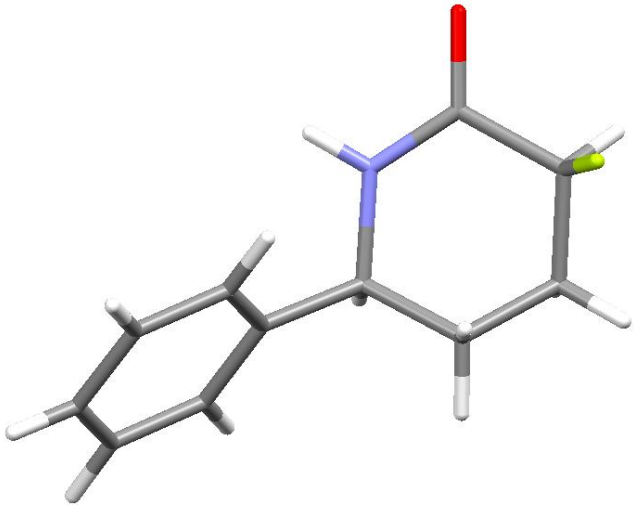

Figure 34 *– DOMJUM is an example of a secondary lactam derivative. It has an F-C-C=O bond torsion angle of 74 °.*

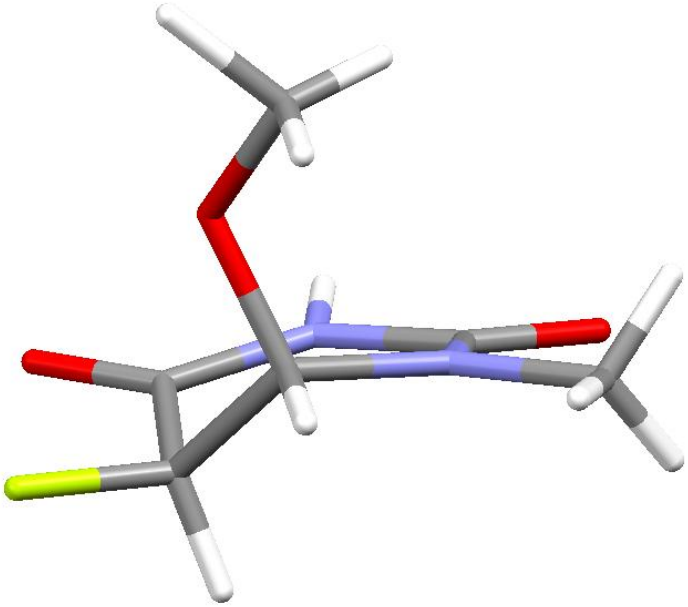

Figure 35 *– MFXHUR exhibits ring puckering that could lead to a lower F-C-C=O torsion angle.*

A1.3.9. Further Example of α-Fluorodiamides

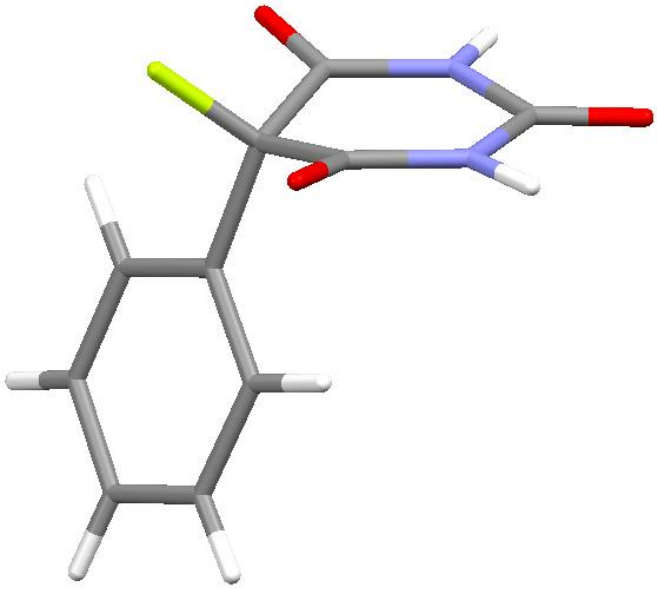

Figure 36 *– HEKTOG is a cyclic fluorodiamide that exhibits gauche F-C-C=O torsion angles.*

A1.3.10. Example of a Tertiary α-Fluoroamide on a Ring

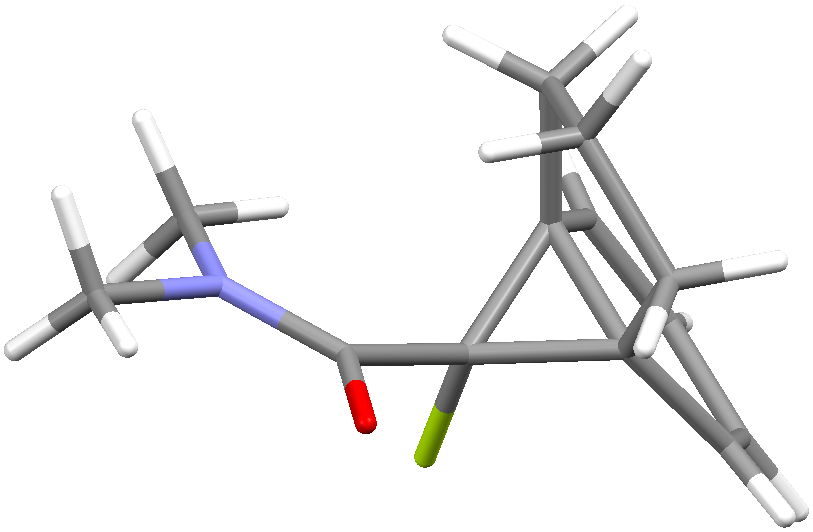

Figure 37 *– AXUCAX is an example of a tertiary fluoroamide derivative with the fluorine atom on a ring system. It has an F-C-C=O bond torsion angle of 100^{o}.*

A1.3.11. Exclusions from α-Fluoroketone Search

The substructure search does not specify non-metal atoms bonded to the unlabelled carbon atom adjacent to the carbonyl carbon, unlike the other fluorocarbonyl moiety searches. In this instance it was observed that the CSD search functions severely limited the number of hits identified when 'NM' was specified despite the fact that the omitted hits did not contain metal atoms at this position. The 143 results analysed are non-metallic structures despite the apparent lack of specificity in the substructure search. This highlights an interesting limitation to the current CSD search functions.

FULBUL exhibits both ketone and acetophenone moieties and so appears twice in the following categories.

Ten of the hits were excluded from the analysis. Eight hits reported no 3D data and so were unusable (BUYYEZ, HAQXEE, IQURAN, IQURER, IQURIV, REYNEQ01, TEFVEF and WAJQIH). SEQQEC showed disorder of the fluorine atom over two sites (***Figure 38***).

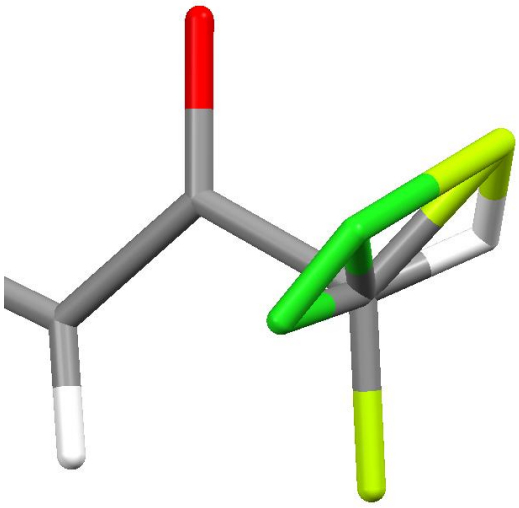

Figure 38 *– SUQQEC exhibits disorder of the fluorine and chlorine atoms adjacent to the ketone moiety.*

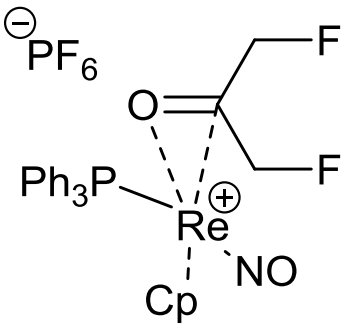

Figure 39 *– The structure of KIZBAW.*

KIZBAW features a simple ketone moiety with two adjacent fluorine atoms – 1,3-difluoroacetone. This molecule is coordinated to a rhenium centre. Although, strictly speaking, the carbon atoms are not bonded to a metal centre, the C=O bond appears to coordinate to the metal and is forced out of plane such that this entry has been excluded from this study. The C=O bond from the sp^2 carbon centre lies 38^o out of plane. ***Figure 40*** shows the C-C-C plane highlighted in red and the C=O bond forced out of plane by 38^o due to interactions with the rhenium atom (blue atom, bottom left of the figure).

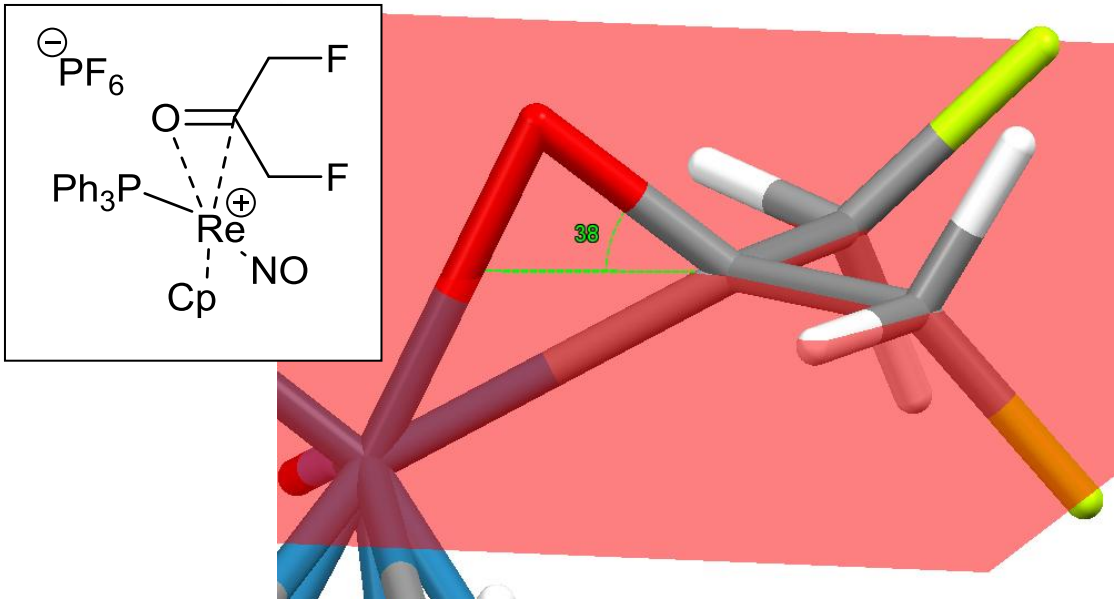

Figure 40 – *KIZBAW exhibits severe distortion of the sp^2 centre by interactions with the coordinated rhenium atom.*

A1.3.12. Further Examples of α-Fluorodiesters

The unsubstituted fluoromalonate (FUGDOC, ***Figure 41***) and the 2-methyl substituted fluoromalonate (15srv211, ***Figure 42***) have near identical torsion angles, suggesting that the addition of the small methyl group has little effect on the overall packing arrangement in the crystal structure. The diphenylmethyl substituted fluoromalonate derivative (14srv277, ***Figure 43***) also shows significant *syn*, *syn* character with F-C-C=O torsion angles of 6^{o} and -14^{o}.

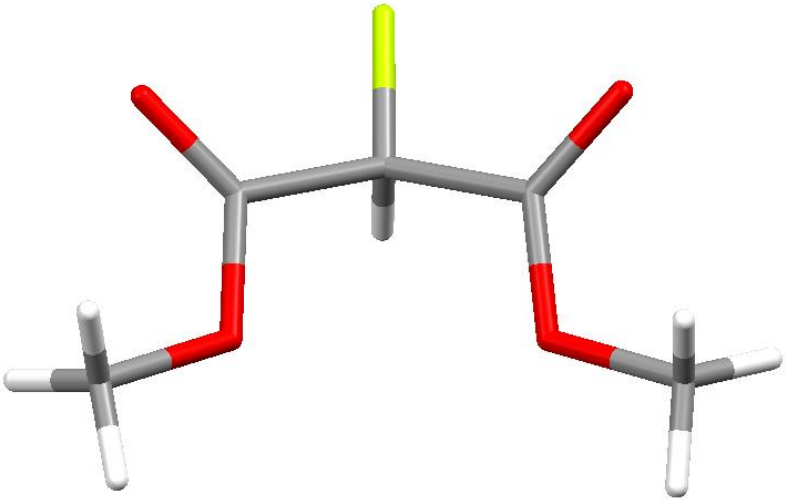

Figure 41 *– The molecular structure of FUGDOC, as determined by X-ray crystallography.*

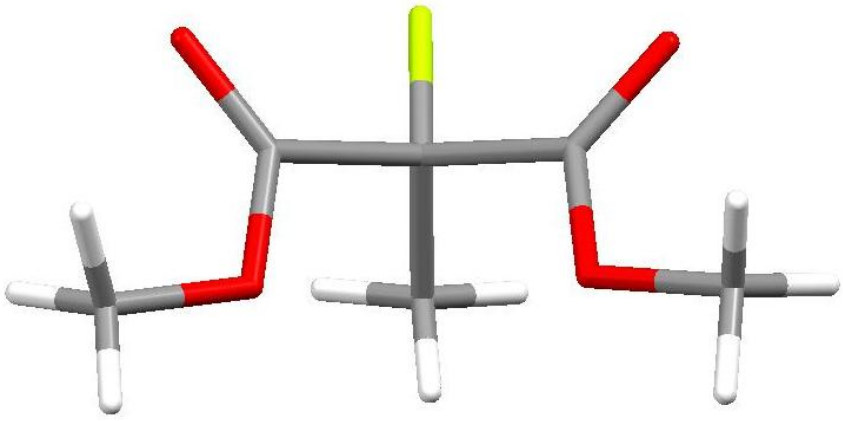

Figure 42 – *The molecular structure of 15srv211, as determined by X-ray crystallography.*

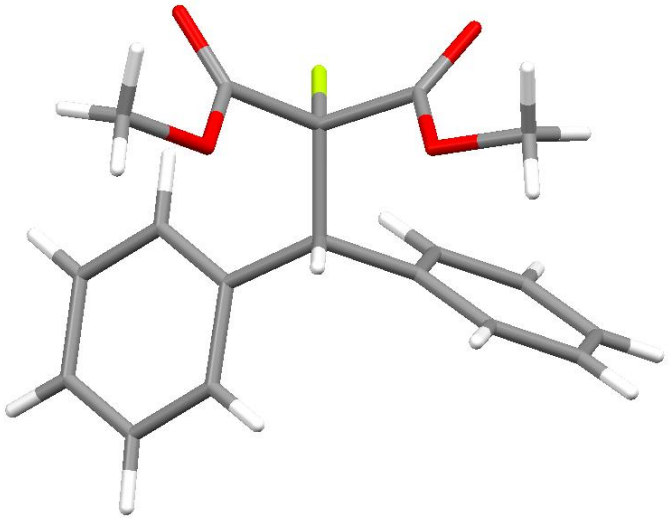

Figure 43 *- The molecular structure of 14srv277, as determined by X-ray crystallography.*

UGOCIE exhibits both intermolecular and intramolecular interactions involving the nitro group and the ester moieties. The carbonyl moiety of the gauche ester is involved with intramolecular interactions with the nitro group and the alkyl moiety of the *syn* fluoroester (with an unusually high torsion angle) is involved with intermolecular interactions with the nitro group and an ester carbonyl oxygen (***Figure 44***).

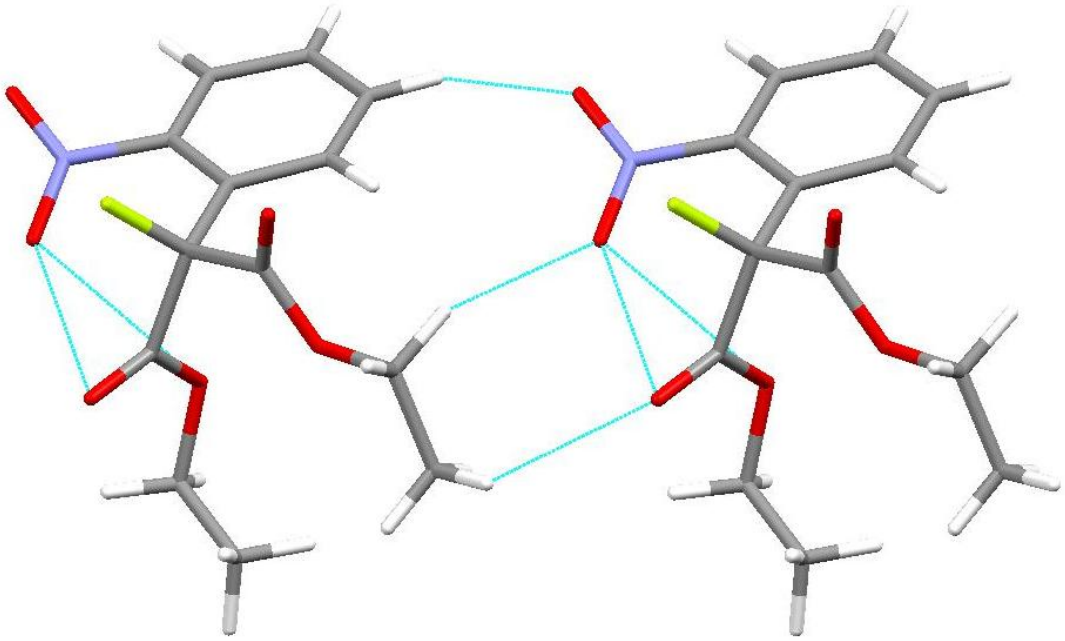

Figure 44 *– The molecular structure of UGOCIE.*

Nitro groups tend to stack in the crystal structure, often alternating between nitrogen and oxygen atoms. Phenyl rings often pi stack and so the addition of a nitrophenyl moiety to a molecule would seem to be a key factor in the determination of the crystal packing interactions. 15srv034 shows extensive nitrophenyl stacking interactions (***Figure 45***).

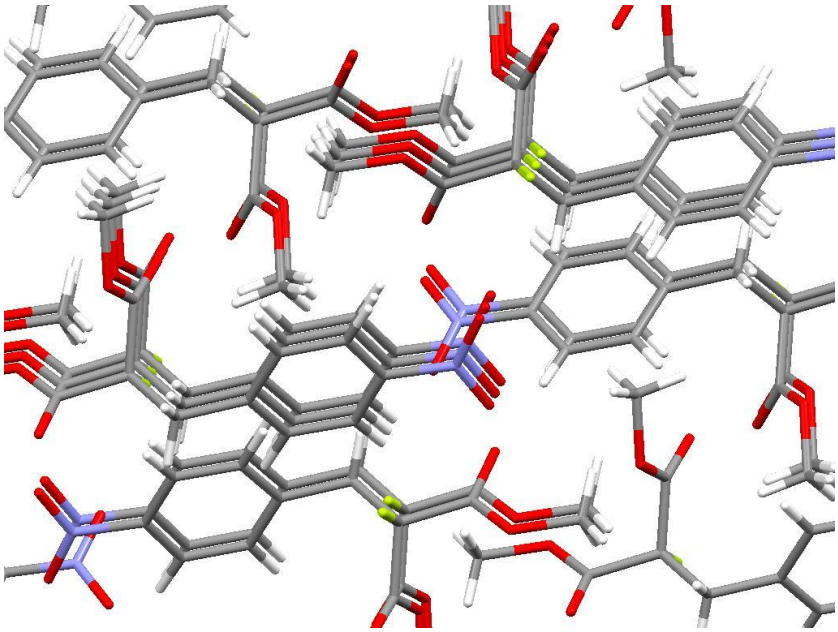

Figure 45 – *The crystal structure of 15srv034 showing extensive stacking of the nitro and phenyl moieties.*

Other interactions involving the nitro moiety are also observed. MUQBEH exhibits attractive intramolecular interactions between the carbonyl oxygen of the eclipsed fluoroester moiety and the nitrogen of the adjacent nitro group. Repulsive intramolecular interactions are also observed between the *syn* fluoroester moiety and an adjacent ester carbonyl moiety which could account for the larger than usual *syn* torsion angles of -25^{o} (MUQBEH (A)) and -27^{o} (MUQBEH (B)) (***Figure 46***).

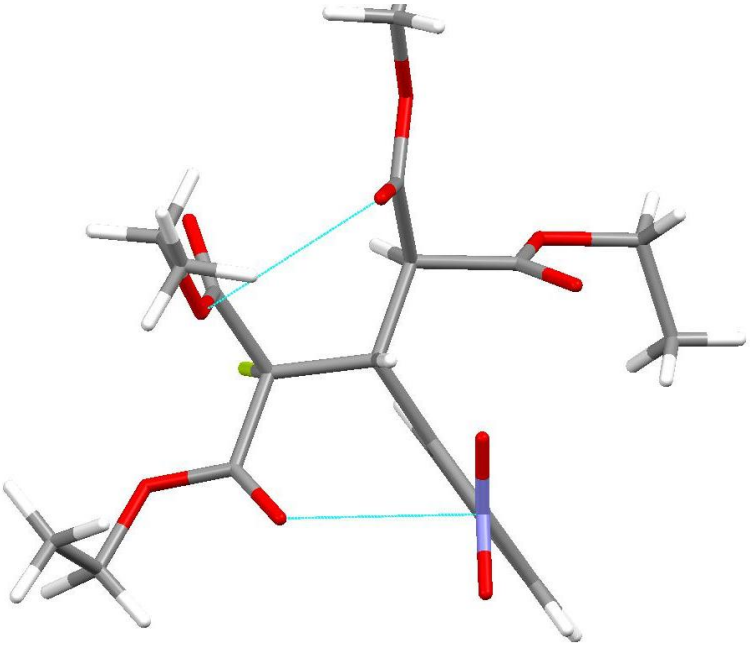

***Figure 46** – The molecular structure of MUQBEH.*

Bibliography

[1] Harsanyi, A.; Sandford, G. *Org. Process Res. Dev.* **2014**, 18, 981-992.
[2] Bergmann, E.; D.; Cohen, S.; Shani, A. *Isr. J. Chem.* **1963**, 79-85.
[3] Koelsch, C. F. *J. Am. Chem. Soc.* **1943**, 65, 2458-2459.
[4] Albertson, N. F.; Fillman, J. L. *J. Am. Chem. Soc.* **1949**, 71, 2818-2820.
[5] Ansell, M. F.; Hey, D. H. *J. Chem. Soc.* **1950**, 1683-1686.
[6] Michael, J. P.; de Koning, C. B.; van der Westhuyzen, C. W.; Fernandes, M. A. *J. Chem. Soc. Perkin Trans. 1* **2001**, 2055-2062.
[7] Hong, S.; Kim, M.; Jung, M.; Ha, M. W.; Lee, M.; Park, Y.; Kim, M.; Kim, T.; Lee, J.; H. Park, H. *Org. Biomol. Chem.* **2014**, 12, 1510–1517.
[8] Reddy, D. S.; Shibata, N.; Nagai, J.; Nakamura, S.; Toru, T.; Kanemasa, S. *Angew. Chem. Int. Ed.* **2008**, 47, 164–168.
[9] Maligres, P. E.; Chartrain, M. M.; Upadhyay, V.; Cohen, D.; Reamer, R. A.; Askin, D.; Volante, R. P.; Reider, P. J. *J. Org. Chem.* **1998**, 63, 9548-9551.
[10] Wilent, J.; Petersen, K. S. *J. Org. Chem.* **2014**, 79, 2303-2307.
[11] S. Banerjee, W. J. Wiggins, J. L. Geoghegan, C. T. Anthony, E. A. Woltering and D. S. Masterson, *Org. Biomol. Chem.* 2013, 11, 6307–6319.
[12] Gutman, A. L.; Meyer, E.; Yue X.; Abell, C. *Tetrahedron Lett.* **1992**, 33, 3943–3946.
[13] Atkinson, F. L.; Barker, M. D.; Douault, C.; Garton, N. S.; Liddle, J.; Patel, V. K.; Preston, A. G. S.; Wilson, D. M. US2013/0040984 A1, **2013**.
[14] Curtis, N. R.; Davies, S.; Gray, M.; Leach, S. G.; McKie, R. A.; Vernon L. E.; Walkington, A. *Org. Process Res. Dev.* **2015**, 19, 865–871.
[15] Willis, N.; Fisher, C.; Alder, C. M.; Harsanyi, A.; Shukla, Lena; Adams, J. P.; Sandford, G. *Green Chem.* **2016**, *18*, 1313-1318.